Chem Rev Lett 6 (2023) 128-138

Research Article

Chemical Review and Letters
journal homepage: www.chemrevlett.com
ISSN (online): 2645-4947 (print) 2676-7279

Adsorption of a biological active ethionamide over the Surface of a Fe- porphyrin induced carbon nancone (Fe-PICNC) system Through a Density Functional Theory (DFT)

Anupam Yadav[1], Ali Taha[2], Yousra Ali Abdulsayed[3], Shakir Mahmood Saeed[4,*]

[1] *Department of CEA, GLA University, Mathura, India*
[2]*Pharmacy college, Al-Farahidi University, Iraq*
[3]*Department of Optical Techniques, Al-Zahrawi University College, Karbala, Iraq*
[4]*Department of Pharmacy, Al-Noor University College, Nineveh, Iraq*

ARTICLE INFO

Article history:
Received 25 February 2023
Received in revised form 19 July 2023
Accepted 19 July 2023
Available online 10 August 2023

Keywords:
Adsorption
Porphyrin
Etionamide
DFT calculations
Optimization

ABSTRACT

This study used Density Functional Theory (DFT) calculations to investigate the adsorption behavior of ethionamide (ET) on Fe-porphyrin induced carbon nanocones (Fe-PICNCs). The B3LYP method with the 6-31G* basis set was employed to determine total energies, physical parameters, and electronic analysis. Results indicated that the ET molecule strongly adsorbs onto Fe-PICNCs, with adsorption energies ranging from -30.96 to -15.00 kcal/mol, indicating very strong chemical interactions. The findings suggest that Fe-PICNCs are effective adsorbents for removing unwanted ET drug emissions from the environment. The energy gap (work function) of isolated Fe-PICNCs was calculated as 2.00 eV (3.82 eV). ET adsorption had an insignificant effect on the energy gap (work function) of the Fe-PICNC structures, indicating that they cannot be used as electronic conductivity type or work function type sensors for the ET drug.

1.Introduction

Ethionamide (ET) is a compound with molecular formula of $C_8H_{10}N_2S$ which is a drug used for pulmonary tuberculosis and extra-pulmonary tuberculosis. The ET drug fits to a group of the drugs named antibiotics. A number of scientists recently have interested in the environmental effects of the drugs that gathered in the environment in large amounts and their side effects on living organisms are dangerous which should be important the investigation of this matter [1, 2]. In many studies, more than 70 drugs have been found as the drug contaminants in soil and water of different countries [3, 4]. The Drug accumulated in the environment affect health of human, animal, and plants [5-8]. It is necessary that the accumulated drugs should be identified by a sensor to find where the drug gathered. Nanoparticles are the materials that can be used as the sensors for the identification of the released drugs [9, 10]. These nanoparticles have received much attention as chemical sensors and other applications as drug delivery, batteries and catalysts [11-13]. Graphene is provided by a variety of methods, such as chemical vapor deposition (CVD) mechanical exfoliation, chemical production, epitaxial growth on silicon carbide (SiC) [14-16].

Porphyrins are important aromatic macrocycle organic structures that play a vital role in biological functions such as respiration, electron transport, and photosynthesis [17-19]. These structures consist of four functionalized pyrroles connected by methine bridges

∗ Corresponding author.; e-mail: shakir.mahmood@alnoor.edu.iq
https://doi.org/ 10.22034/crl.2023.387354.1204

(=CH-). Porphyrins and their related compounds have a wide range of applications in medicine, the energy sector, and the chemical industry [20]. Because of their strong light absorption capabilities, porphyrins are being studied for their potential use in non-invasive cancer treatment through photodynamic therapy (PDT), as well as for their potential as anticancer and antioxidant materials [21-23]. Metalloporphyrins are porphyrin cycles that have metal ions inserted into them and have been extensively studied as catalysts in organic synthesis, oxidation of organic compounds, photocatalytic water splitting, and dye-sensitized solar cells [24-27]. They have also been evaluated for use in chemical sensors, such as detecting trace amounts of TNT vapors and volatile organic compounds in human breath [28-33]. Carbon nanomaterials have also attracted significant interest among researchers due to their exceptional properties and high surface area, making them useful for a wide range of applications, including gas adsorption, detection, and catalysis [34-42].

The manuscript explores the potential of Fe-porphyrine-induced carbon nanocone (Fe-PICNC) as a sensing material for identifying and adsorbing the ET drug, using DFT calculations. The findings of this study have significant implications for the development of an effective adsorbent for the ET drug, as well as for designing a ssionsuitable sensing mechanism.

2.Computational Details

This study employed the DFT method at the B3LYP/6-31G(d) theoretical level, utilizing GAMESS programs for all calculations [43]. The B3LYP method is commonly used in the study of materials based on nanostructures [44-46]. Moreover, a review of the literature suggests that it is a dependable and appropriate density functional for predicting the energetic, electronic, structural, and optical properties of various nanostructures [47-53]. The DFT method is one of the most powerful approaches for quantum calculations.

During the optimization process, desirable molecular structures are optimized to reach the minimum energy, and the energy of the targeted systems is subsequently computed [54] To introduce a defect in the carbon nanocone, a PI ring consisting of 4 nitrogen atoms and 20 carbon atoms was added at the apex of the cone, resembling the structure of PI. The Gaussview software was employed to substitute the PI structure with the defect in the carbon nanocones (PICNC).

Optimization calculations were conducted for both the complete Nanocone and the PICNC structure. Finally, the GaussSum program was used to generate DOS plots [55]. The adsorption energy (E_{ads}) is calculated as follows:

$$E_{ads}=E_{(drug/adsorbent)}-[E_{(adsorbent)} + E_{(drugt)}]+ E_{BSSE} \quad (1)$$

The adsorption energy of an ET molecule onto a Fe-PICNC molecule is denoted by the term Eads. Specifically, $E_{(drug)}$ represents the energy of the ET molecule, while $E_{(adsorbent)}$ is the total energy of the Fe-PICNC molecule. The total energy of the adsorbed ET molecule on the surface of the Fe-PICNC molecule can be expressed as $E_{(drug/adsorbent)}$. Additionally, the Basis Set Superposition Error (BSSE) is accounted for using the counterpoise method [56], and in this study, we evaluate some interaction indicators that are useful for analysis. In this study, the Natural Bond Orbitals (NBO) charge analysis [57] was conducted at the same level of theory. The HOMO-LUMO energy gap (E_g) is defined as:

$$E_g = E_{LUMO}-E_{HOMO} \quad (2)$$

The E_{HOMO} and E_{LUMO} orbitals represent the energy levels of the highest occupied and lowest unoccupied orbitals, respectively. It is typical to assume that the Fermi level (E_F) is positioned near the center of the molecule's energy gap (E_g) at 0 K.

3.Results and Discussions

3.1. Optimizing the Geometry of Pristine Carbon Nanocones (CNC) and Porphyrin-Induced Carbon Nanocones (PICNCs)

In our calculations, we observed a low energy gap value (0.59 eV) between the HOMO and LUMO levels in the carbon nanocone (CNC) structure. However, replacing the porphyrin ring in a CNC resulted in a slight increase in the energy gap value (1.22 eV) (Table 1), indicating a potential for the modified structure to act as a semiconductor. Despite this change, the binding energy and overall stability of the system remained relatively unchanged. After optimization calculations on the substituted porphyrins in the carbon nanocone (PICNC), we found that the resulting hole size is suitable for accommodating different metals.

We anticipate that binding the nitrogen atoms in the cavity with the atoms of the transition metals could effectively prevent clustering of these metals. The results of the optimization calculations, encompassing the energy levels of the HOMO and LUMO orbitals, the energy gap (E_g) between them, Fermi level energy, bipolar moment, and work function, are presented in Table 1.

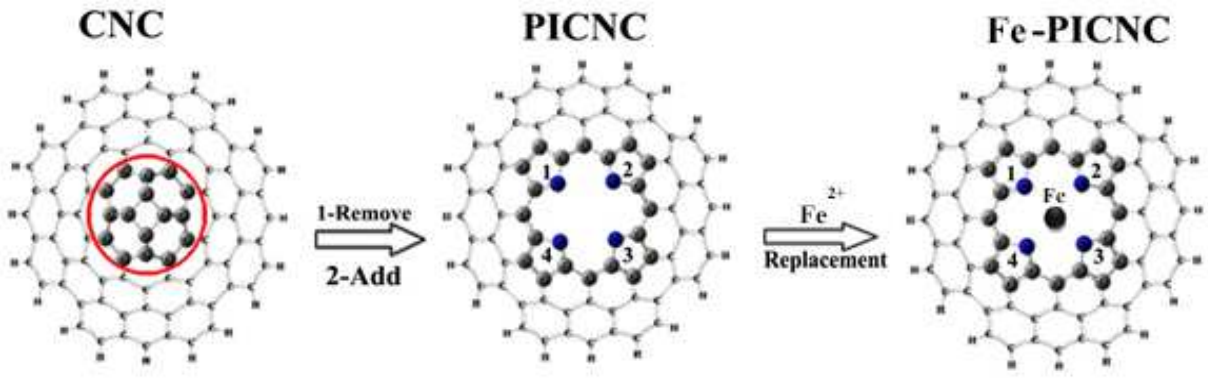

Fig 1. A schematic formation of porphyrins and Fe-porphyrins-induced in carbon nanocones.

Table 1: Energy of HOMO and LUMO orbitals, energy difference of HOMO and LUMO orbitals (E_g), Fermi level energy (E_F), bipolar moment (DM) and working function (Φ) for ethionamide molecule (ET), carbon nanocone (CNC), porphyrins-induced carbon nanocone (PICNC), and Fe-PICNC at the theoretical level of B3LYP/6-31G(d)

Systems	E_{HOMO}(eV)	E_F(eV)	E_{LUMO}(eV)	E_g(eV)	DM(Debye)	Φ
ET	-5.78	-3.46	-1.15	4.63	-	3.60
CNC	-3.98	-3.68	-3.39	0.59	7.79	3.68
PICNC	-5.00	-4.39	-3.78	1.22	10.35	4.39
Fe-PICNC	-4.82	-3.82	-2.82	2.00	7.80	3.82

.

3.1. Investigating the effects of Fe-porphyrin-induced on the *structure of carbon nanocone (Fe-PICNC)*

Fe^{2+} can be located at the center of the porphyrin central cavity depending on its size. To investigate how porphyrin-induced defects affect carbon nanocones, divalent iron ion substituted at the center of porphyrin molecules from the transition elements in carbon nanocones. The team then performed optimization calculations for three models, namely, the carbon nanocone (CNC), the porphyrin ring-induced model (PICNC), and the Fe-porphyrin-induced model in carbon nanocones (Fe-PICNC), as illustrated in Fig 1. These calculations aimed to identify the structural changes resulting from these modifications.Table 1 presents evidence that the HOMO and LUMO orbitals of Fe-PICNC, a type of porphyrin-induced carbon nanocone, undergo alterations when a Fe ion is inserted into the molecule's vacant cavity. Notably, replacing the Fe cation in the porphyrin central cavity leads to a significant increase in E_g as compared to isolated PICNC (as shown in Table 1). These findings imply that the introduction of a Fe cation into PICNC induces a shift in the energy levels between the HOMO and LUMO orbitals, which suggests the emergence of new HOMO and LUMO orbitals with lower energy levels. The TDOS diagram of Fe-PICNC has been shown in Fig 2, too. The absorption of Fe^{2+} causes a shift in the Fermi level. The energy gap of the porphyrin molecule in the carbon nanocone is approximately 1.22 eV, indicating that the compound exhibits semiconductor characteristics. Changes to the Fermi level of a semiconductor due to the absorption
of metal ions can modify the field emission currents. The carbon nanocone being studied has a conjugated structure, resulting in low polarity. However, by creating a cavity and adding nitrogen with high electronegativity, the dipole moment vector in this structure will be oriented towards the nitrogen atoms, resulting in higher polarity (See Table 1). On the other hand, by placing Fe cation with lower electronegativity than nitrogen in the empty cavity, the polarity becomes

neutral, and as a result, the dipole moment decreases. As seen from Table 1, placing a Fe ion at the center of the cavity equals 7.80 Debye in comparison; the dipole moment of PICNC equals 10.35 Debye.

3.2. Adsorption of ET molecule on Fe-PICNC

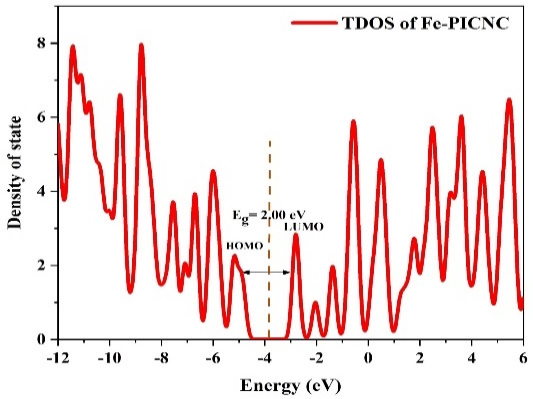

Fig 2. TDOS diagram of Fe-PICNC structure.

Our study investigated the interaction between the ET molecule and Fe-PICNC. To determine the most favorable adsorption energy, we analyzed how the ET molecule interacts with the Fe cation within Fe-PICNC from external sites.

Fig 3 illustrates the ET molecule interacting with Fe-PICNC, with the ET molecule located at the center of the porphyrin ring from an external site. DFT calculations using the B3LYP method and 6-31G(d) basis set were conducted to investigate the electrostatic properties of the ET molecule and the outer surfaces of Fe-PICNC. We conducted scans of various dihedral angles to identify the most stable adsorption configuration (as shown in Fig 3). Table 2 presents the E_{ads} values computed using Equation (1) for the adsorption of ET onto Fe-PICNC molecules.

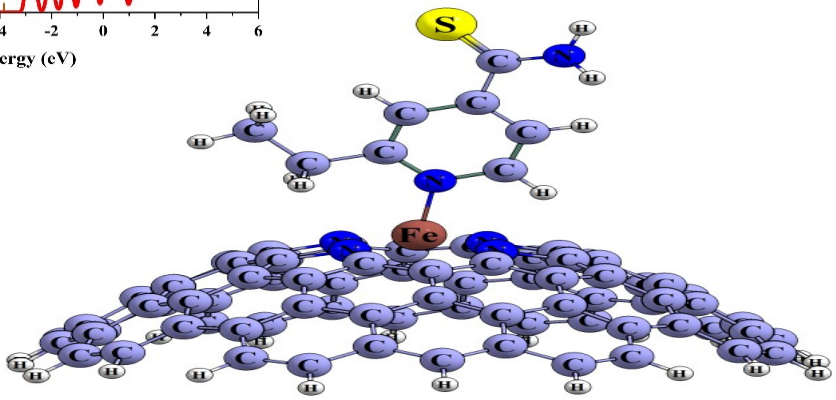

S1

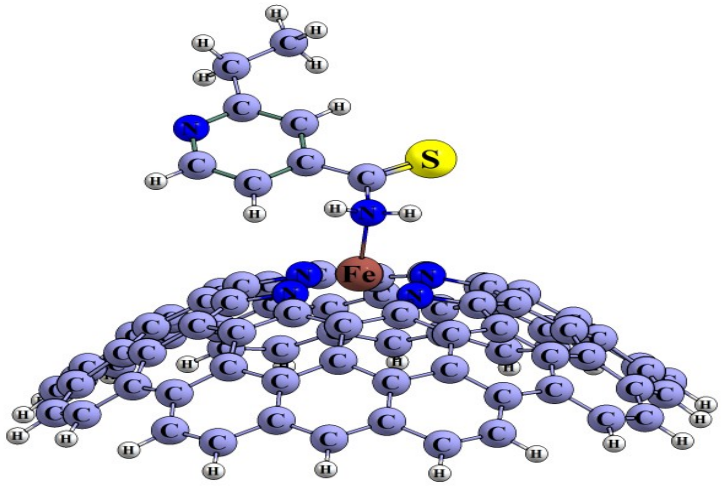

S2

S3

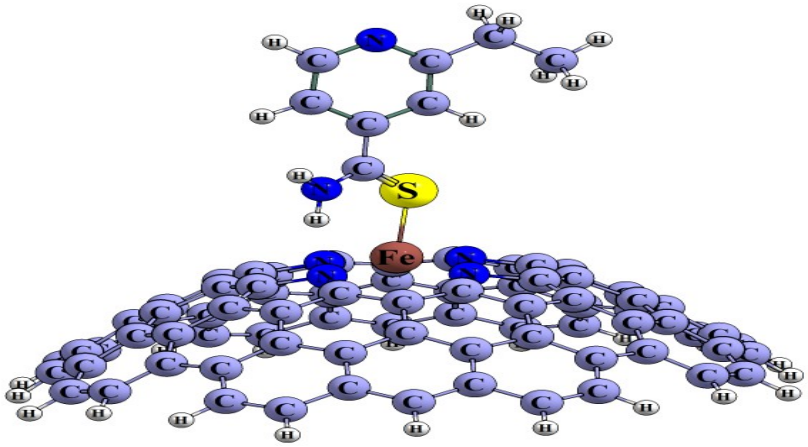

Fig 3. Optimized structures for the adsorption of ET molecules from the outer surface of Fe-PICNC.

Table 2. Absorption energies (E_{ads}), energy of HOMO and LUMO orbitals, energy difference of HOMO and LUMO orbitals (E_g), Fermi level energy (E_F), and dipole moment (DM) and working function for (Fe-PICNC) after adsorption of ET molecule at the theoretical level.

Systems	E_{ads} (kcal/mol)	E_{HOMO} (eV)	E_F (eV)	E_{LUMO} (eV)	E_g (eV)	$\%\Delta E_g$	DM (Debye)	Φ (eV)	$\%\Delta\Phi$
S1	-30.96	-4.71	-3.71	-2.71	2.005	0.25	4.20	3.71	-2.92
S2	-23.76	-4.76	-3.76	-2.76	2.002	0.1	6.39	3.76	-1.71
S3	-15.00	-4.78	-3.80	-2.82	1.955	-2.25	4.89	3.80	-0.59

Table 2 shows that following optimization, three stable adsorption configurations were observed, where the ET molecule is in contact with Fe-PICNC structure. These configurations are: S1) the S atom of ET molecule is bonded with Fe atom of the external surface of Fe-PICNC structure, S2) the N atom of pyridine ring is bonded with Fe atom of Fe-PICNC structure, and S3) the N atom of amine group is bonded with Fe atom of Fe-PICNC. The adsorption energies (E_{ads}) for each configuration were also determined and are listed in Table 2 as -30.96, -23.76, and -15.00 kcal/mol for S1, S2, and S3 configurations, respectively.

The negative adsorption energy values in Table 2 indicate that the structures are stable due to a very strong chemisorption interaction between the ET molecule and Fe-PICNC. This suggests that the ET molecule can interact with the Fe atom in Fe-PICNC structures via its S, N (pyridine), or amine groups, resulting in stable configurations (as shown in Fig 3). The S-Fe and N-Fe interaction distances for these configurations are 2.213, 1.895, and 1.986 □, respectively (as listed in Table 3). Fe-N bond lengths in Fe-PICNC increase after ET adsorption, as shown in Table 3. Therefore, Fe-PICNC can be used as a suitable adsorbent for removing unwanted ET drug emissions in the environment.

Table 3. Bond length and angle bonds obtained from optimization calculations at the theoretical level B3LYP/6-31G(d) related to Fe-PICNC after ET molecule adsorption process

Systems	Fe-N1	Fe-N2	Fe-N3	Fe-N4	Fe-ETH
Fe-PICNC	1.947	1.948	1.947	1.948	-
S1	2.023	1.978	1.993	1.977	2.213
S2	2.002	2.003	2.010	2.009	1.895
S3	2.003	1.993	1.980	1.982	1.986

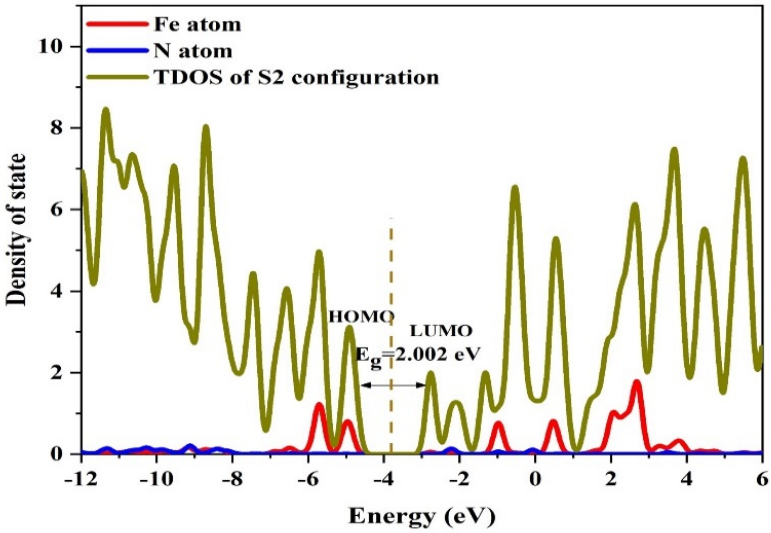

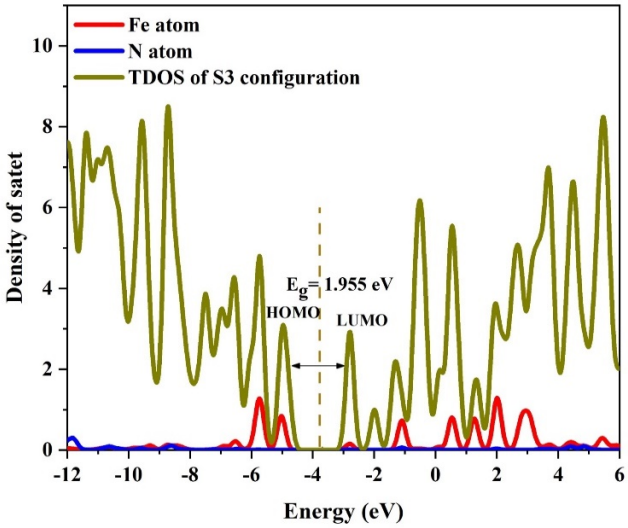

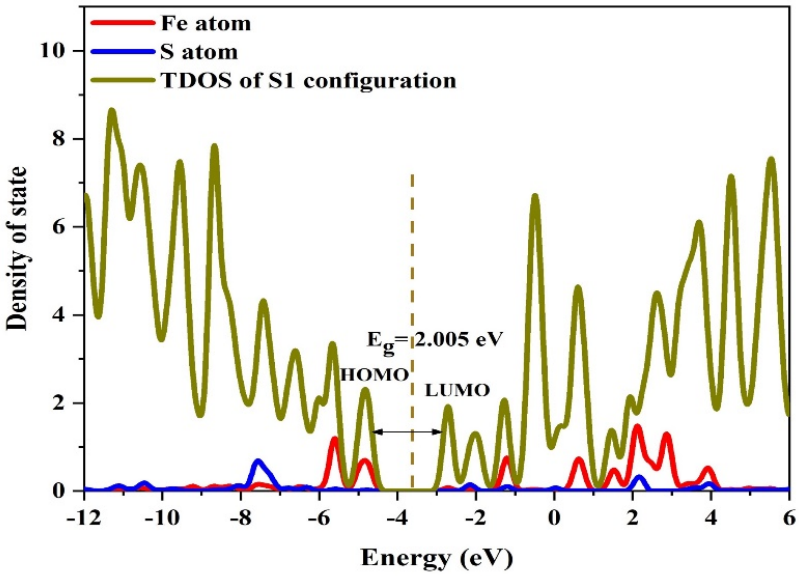

Fig 4. Total density of states (TDOS) and partial density of states (PDOS) of S1, S2, and S3 configurations (The dash line shows Fermi level).

.

The electronic properties, specifically E_{HOMO}, E_{LUMO}, and E_g, were also investigated in our study. These parameters are important in explaining the behavior of molecules. Table 2 shows that the change in E_g for the configurations resulting from ET adsorption on the outer surface of Fe-PICNC, compared to the respective adsorbents, is insignificant (%ΔE= 0.25, 0.1, and -2.25). The negligible change in E_g is due to the HOMO and LUMO levels of these configurations remaining unchanged compared to their adsorbents. We also analyzed the electronic properties of Fe-PICNC after ET adsorption in three configurations, as presented in Table 2 and Fig 4.

lts show an insignificant change in the TDOS of the considered configurations compared to Fe-PICNC. Specifically, we did not observe new LUMO and HOMO levels in these configurations compared to Fe-PICNC. Furthermore, the TDOS and PDOS plots confirm that the valence and conduction levels in S1, S2, andconfigurations did not shift notably, leading to an insignificant change in the E_g value. According to the PDOS diagrams, HOMO and LUMO of these configurations consist of valence orbitals of Fe atom of Fe-PICNC.

When it comes to detecting potential, there are two key factors to consider: E_{ads} and E_g. If the Eads falls within a certain range, the adsorption of the ET molecule onto Fe-PICNC can be reversed. However, stronger interactions are not ideal for sensing ET because they result in longer recovery times and make it harder to remove the drug molecule from Fe-PICNC. This relationship can be mathematically expressed as follows: [58, 59]:

$$\tau = \nu_0^{-1} \exp(-E_{ads}/kT) \quad (3)$$

The equation given establishes a relationship between recovery time (τ) and attempt frequency (ν_0), and the physical parameters of temperature (T) and Boltzmann constant (k). [60]. Equation (3) demonstrates an exponential correlation between E_{ads} and recovery time, indicating that as E_{ads} increases, the recovery time for the sensor also increases. Sensor recovery is a crucial process that can be performed at room temperature or higher, as suggested by some sources. [61]. The sensing ability of Fe-PICNC is also impacted by another crucial parameter, namely the HOMO-LUMO energy gap (E_g) in the presence of the ET molecule. Equation (4) demonstrates that E_g is directly proportional to the population of conduction electrons (σ), which increases when ET is adsorbed onto Fe-PICNC, leading to a reduction in the HOMO-LUMO energy gap (E_g). In contrast, increasing the value of $\%\Delta E_g$ also enhances the sensing potential. The relationship between E_g and the electrical conductance of nanoparticles can be mathematically expressed as follows:

$$\sigma = A\, T^{3/2} \exp(-E_g/2kT) \quad (4)$$

The equation includes a constant A (measured in electrons/$^{m3}K^{3/2}$) and the Boltzmann constant k. Moreover, the outcomes obtained through this method exhibit a clear correlation with the experimental methods described in the scientific literature. [62].

Based on the information presented in Table 2, the adsorption of the ET drug did not modify the energy gap of Fe-PICNC sufficiently to produce a notable change in its electronic conductivity. The findings suggest that Fe-PICNC/ET may only be considered as a viable option for chemical adsorption materials that can eliminate unwanted ET drugs released into the environment.

3.3. Work function analysis

In the electronics industry, a crucial task is to regulate the work function of materials to improve device performance. Managing surface properties by controlling the work function of nanomaterials is particularly important. Our investigation focused on the changes in work function resulting from charge transfer between the adsorbent (Fe-PICNC) and the adsorbate (ET molecule). In the case of a semiconductor molecule, the work function represents the minimal energy necessary to remove an electron from the Fermi surface to a location far enough from the material's impact. Additionally, the following classical equation provides a theoretical description of the current density of electrons emitted in a vacuum:

$$j = AT^2 \exp\left(\frac{-\Phi}{kT}\right) \qquad (5)$$

The equation that describes the current density of electrons emitted in a vacuum is associated with a constant known as Richardson's constant (A/m^2). In this equation, T denotes the temperature in degrees Kelvin, and (eV) is a function of the material. The value of this constant can be determined using the following mathematical formula::

$$\Phi = E_{inf} - E_F \qquad (6)$$

Einf represents the electrostatic potential at infinity, while EF denotes the Fermi level energy. Assuming E_{inf} to be zero, Table 2 provides the computed values of the function using Equation (6) for the Fe-PICNC molecule upon interaction with ET. Based on DFT calculations, the values of Fe-PICNC molecules were altered upon ET adsorption. Equation (5) indicates that the electron diffusion current density is negatively dependent on an exponential value. Since the Fermi level of Fe-PICNC is not significantly affected, the current density undergoes a slow change upon ET adsorption, suggesting low sensitivity of the adsorbent to the presence of ET. The %ΔΦ values of Fe-PICNC after ET adsorption in three configurations are -2.92, -1.71, and -0.59, respectively, indicating a reduced sensing ability. Therefore, Fe-PICNC may not be suitable to function as an Φ-type sensor.

3.4. NBO Analysis

The NBO analysis, as shown in Table 4, involved assessing all feasible interactions between filled Lewis-type NBOs (donors) and empty non-Lewis NBOs (acceptors). These interactions, referred to as delocalization corrections, were incorporated to refine the natural Lewis structure of zeroth-order. The table presents the stabilization energies ($E^{(2)}$) for the most significant interaction between electron-donor orbitals (i) and electron-acceptor orbitals (j). A high $E^{(2)}$ value suggests a robust interaction between the Fe metal ion and the PICNC molecule, indicating their potential to transfer electrons from the donor orbital (i) to the acceptor orbital (j).

Table 4. Part of the second-order perturbation of the stabilizing energy calculated for the donor-acceptor natural orbitals for Fe-PICNC, S1, S2, and S3 configurations.

System	Donor NBO (*i*)	Acceptor NBO (*j*)	$E^{(2)}$ (kcal/mol)
Fe-PICNC	LP N(97)	LP* Fe	42.30
	LP N(98)	LP* Fe	42.30
	LP N(99)	LP* Fe	42.28
	LP N(100)	LP* Fe	42.28
S1	LP S	LP* Fe	32.40
	LP S	LP* Fe	33.51
	LP S	LP* Fe	44.70
	LP S	LP* Fe	111.78

S2	LP N(Py)	LP* Fe	41.32
	LP N(Py)	LP* Fe	46.80
	LP N(Py)	LP* Fe	23.42
S3	LP N(amine)	LP* Fe	55.44
	LP N(amine)	LP* Fe	18.60
	LP N(amine)	LP* Fe	3.55

To gain further insight, we conducted an analysis of the degree of stabilization energy ($E^{(2)}$), electron donor orbitals (i), and electron acceptor orbitals (j) when the ET molecule is in proximity to the Fe metal ion. Our findings suggest that the key electron donor orbitals (i) and electron acceptor orbitals (j) that result in high stabilization energy are LP_S => LP^*_{Fe}, $LP_{N(Py)}$ => LP^*_{Fe}, and $LP_{N(amine)}$ => LP^*_{Fe} for S1, S2, and S3, respectively. In these interactions, the lone pair electrons of the S and N atoms transfer to the lone pair anti-bonding orbital of the Fe metal ion, which is in line with the outcomes obtained from FMO analysis.

4. Conclusion

We employed Density Functional Theory (DFT) to investigate the adsorption of an ET molecule on Fe^{2+} ion porphyrin induced carbon nanocone (Fe-PICNC) for removing unwanted ET molecule drug from the environment. The results revealed that the Fe molecule is adsorbed on Fe-PICNC with adsorption energies ranging from -30.96, -23.76, -15.00 kcal/mol in S1, S2, and S3 configurations, respectively. The ET molecule showed the strongest interaction when the S atom of ET molecule interacted with Fe from Fe-PICNC with E_{ads} = -30.96 kcal/mol. The energy gap (E_g) of S1, S2, and S3 configurations showed negligible changes compared to isolated Fe-PICNC. As the conductivity of semiconductors depends on their energy gap energies, since ET adsorption insignificantly changes the energy gap energies of the considered structure, none of the three configurations can be employed as sensible conductivity-type sensors for the ET drug. In determining the sensing ability, two parameters, E_{ads} and E_g, are crucial. The strong chemical absorption of ET gas over Fe-PICNC leading to a significant amount of E_{ads} is unsuitable, while a negligible change in E_g is unfavorable for promising sensing ability. Based on these criteria, Fe-PICNC is just a good candidate for detecting and removing the unwanted ET drug from the environment. Furthermore, the %ΔΦ value for obtained configurations is about -2.92, -1.71, and -0.59, respectively, indicating a lower sensing ability. It is suggested that Fe-PICNC cannot serve as an Φ-type sensor.

References

[1] M. Sayadi, R. Trivedy, R. Pathak, Pollution of pharmaceuticals in environment. *I Control Pollution,* 26 (2010) 89-94.

[2] G.W. Aherne, Immunoassays in the analysis of water. *International journal of environmental analytical chemistry,* 21 (1985) 79-88.

[3] S. Webb, A data-based perspective on the environmental risk assessment of human pharmaceuticals I—collation of available ecotoxicity data. *Pharmaceuticals in the environment: sources, fate, effects and risks,* (2001) 175-201.

[4] D.R. Dietrich, S.F. Webb, T. Petry, Hot spot pollutants: pharmaceuticals in the environment. *Toxicology Letters,* 131 (2002) 1-3.

[5] M. Petrović, S. Gonzalez, D. Barceló, Analysis and removal of emerging contaminants in wastewater and drinking water. *TrAC Trends in Analytical Chemistry,* 22 (2003) 685-696.

[6] O. Jones, N. Voulvoulis, J. Lester, Human pharmaceuticals in the aquatic environment a review. *Environmental technology,* 22 (2001) 1383-1394.

[7] M. Sayadi, Contamination of soil industrial area. *Lambert. Academic. Publishing, Germany,* 156 (2010).

[8] E. Zuccato, D. Calamari, M. Natangelo, R. Fanelli, Presence of therapeutic drugs in the environment. *Lancet.,* 355 (2000) 1789-1790.

[9] W. Baran, E. Adamek, J. Ziemiańska, A. Sobczak, Effects of the presence of sulfonamides in the environment and their influence on human health. *Journal of hazardous materials,* 196 (2011) 1-15.

[10] A. Białk-Bielińska, S. Stolte, J. Arning, U. Uebers, A. Böschen, P. Stepnowski, M. Matzke, Ecotoxicity evaluation of selected sulfonamides. *Chemosphere,* 85 (2011) 928-933.

[11] A.S. Berdinsky, Y.V. Shevtsov, A.V. Okotrub, S.V. Trubin, L.T. Chadderton, D. Fink, J. Lee, Sensor properties of fullerene films and fullerene compounds with iodine. *Chemistry for Sustainable Development,* 8 (2000) 1-146.

[12] Y.-M. Chu, U. Nazir, M. Sohail, M.M. Selim, J.-R. Lee, Enhancement in thermal energy and solute particles

using hybrid nanoparticles by engaging activation energy and chemical reaction over a parabolic surface via finite element approach. *Fractal and Fractional,* 5 (2021) 119.

[13] T. Oku, M. Kuno, H. Kitahara, I. Narita, Formation, atomic structures and properties of boron nitride and carbon nanocage fullerene materials. *Int. J. Inorg. Mater.,* 3 (2001) 597-612.

[14] W. Choi, I. Lahiri, R. Seelaboyina, Y.S. Kang, Synthesis of graphene and its applications: a review. *Critical Reviews in Solid State and Materials Sciences,* 35 (2010) 52-71.

[15] K.E. Whitener Jr, P.E. Sheehan, Graphene synthesis. *Diamond and related materials,* 46 (2014) 25-34.

[16] V. Singh, D. Joung, L. Zhai, S. Das, S.I. Khondaker, S. Seal, Graphene based materials: past, present and future. *Progress in materials science,* 56 (2011) 1178-1271.

[17] T.L. Poulos, Heme enzyme structure and function. *Chem. Rev.,* 114 (2014) 3919-3962.

[18] S. Yoshikawa, A. Shimada, Reaction mechanism of cytochrome c oxidase. *Chem. Rev.,* 115 (2015) 1936-1989.

[19] H. Scheer, An overview of chlorophylls and bacteriochlorophylls: biochemistry, biophysics, functions and applications, Springer(2006).

[20] C.J. Kingsbury, M.O. Senge, The shape of porphyrins. *Coord. Chem. Rev.,* 431 (2021) 213760.

[21] X. Xue, A. Lindstrom, Y. Li, Porphyrin-based nanomedicines for cancer treatment. *Bioconjugate chemistry,* 30 (2019) 1585-1603.

[22] J. Králová, Z. Kejik, T. Briza, P. Poucková, A. Kral, P. Martásek, V. Kral, Porphyrin− cyclodextrin conjugates as a nanosystem for versatile drug delivery and multimodal cancer therapy. *Journal of medicinal chemistry,* 53 (2010) 128-138.

[23] G.D. Bajju, A. Ahmed, G. Devi, Synthesis and bioactivity of oxovanadium (IV) tetra (4-methoxyphenyl) porphyrinsalicylates. *BMC chemistry,* 13 (2019) 1-11.

[24] X. Huang, J.T. Groves, Oxygen activation and radical transformations in heme proteins and metalloporphyrins. *Chem. Rev.,* 118 (2017) 2491-2553.

[25] W. Zhang, W. Lai, R. Cao, Energy-related small molecule activation reactions: oxygen reduction and hydrogen and oxygen evolution reactions catalyzed by porphyrin-and corrole-based systems. *Chem. Rev.,* 117 (2017) 3717-3797.

[26] M. Mojiri-Foroushani, H. Dehghani, N. Salehi-Vanani, Enhancement of dye-sensitized solar cells performances by improving electron density in conduction band of nanostructure TiO2 electrode with using a metalloporphyrin as additional dye. *Electrochimica Acta,* 92 (2013) 315-322.

[27] F. Mendizabal, R. Mera-Adasme, W.-H. Xu, D. Sundholm, Electronic and optical properties of metalloporphyrins of zinc on TiO 2 cluster in dye-sensitized solar-cells (DSSC). A quantum chemistry study. *RSC Adv.,* 7 (2017) 42677-42684.

[28] M.M. Salleh, M. Yahaya, Enriching the selectivity of metalloporphyrins chemical sensors by means of optical technique. *Sens. Actuators. B,* 85 (2002) 191-196.

[29] A. D'Amico, C. Di Natale, R. Paolesse, A. Macagnano, A. Mantini, Metalloporphyrins as basic material for volatile sensitive sensors. *Sens. Actuators. B,* 65 (2000) 209-215.

[30] N.A. Rakow, K.S. Suslick, A colorimetric sensor array for odour visualization. *Nature,* 406 (2000) 710-713.

[31] S. Tao, G. Li, H. Zhu, Metalloporphyrins as sensing elements for the rapid detection of trace TNT vapor. *J. Mater. Chem.,* 16 (2006) 4521-4528.

[32] Y. Amao, I. Okura, Optical oxygen sensor devices using metalloporphyrins. *Journal of Porphyrins and Phthalocyanines,* 13 (2009) 1111-1122.

[33] B.M. Lee, A. Eetemadi, I. Tagkopoulos, Reduced Graphene Oxide-Metalloporphyrin Sensors for Human Breath Screening. *Applied Sciences,* 11 (2021) 11290.

[34] E. Llobet, Gas sensors using carbon nanomaterials: A review. *Sens. Actuators. B,* 179 (2013) 32-45.

[35] R. Gusain, N. Kumar, S.S. Ray, Recent advances in carbon nanomaterial-based adsorbents for water purification. *Coord. Chem. Rev.,* 405 (2020) 213111.

[36] D.J. Babu, D. Puthusseri, F.G. Kühl, S. Okeil, M. Bruns, M. Hampe, J.J. Schneider, SO2 gas adsorption on carbon nanomaterials: a comparative study. *Beilstein journal of nanotechnology,* 9 (2018) 1782-1792.

[37] D.J. Babu, M. Bruns, R. Schneider, D. Gerthsen, J.r.J. Schneider, Understanding the influence of N-doping on the CO2 adsorption characteristics in carbon nanomaterials. *J. Phys. Chem. C,* 121 (2017) 616-626.

[38] F. Ganazzoli, G. Raffaini, Classical atomistic simulations of protein adsorption on carbon nanomaterials. *Current Opinion in Colloid & Interface Science,* 41 (2019) 11-26.

[39] S. Bashiri, E. Vessally, A. Bekhradnia, A. Hosseinian, L. Edjlali, Utility of extrinsic [60] fullerenes as work function type sensors for amphetamine drug detection: DFT studies. *Vacuum,* 136 (2017) 156-162.

[40] E. Vessally, M. Musavi, M.R. Poor Heravi, A density functional theory study of adsorption ethionamide on the surface of the pristine, Si and Ga and Al-doped graphene. *Iranian Journal of Chemistry and Chemical Engineering,* 40 (2021) 1720-1736.

[41] H. Jouypazadeh, S. Arshadi, B.C. Panduro, A. Kumar, S. Habibzadeh, S. Ahmadi, E. Vessally, Metalloporphyrin reduced C70 fullerenes as adsorbents and detectors of ethenone; A DFT, NBO, and TD-DFT study. *Journal of Molecular Graphics and Modelling,* (2023) 108481.

[42] İ. Söğütlü, S. Arshadi, E.A. Mahmood, V. Abbasi, S. Kamalinahad, E. Vessally, In silico investigation of metalophthalocyanine substituted in carbon nanocones (TM-PhCCNC, TM= Sc2+, Cr2+, Fe2+ and Zn2+) as a promising sensor for detecting N2O gas involved in Covid-19. *Journal of Molecular Structure,* 1284 (2023) 135263.

[43] M.W. Schmidt, K.K. Baldridge, J.A. Boatz, S.T. Elbert, M.S. Gordon, J.H. Jensen, S. Koseki, N. Matsunaga, K.A. Nguyen, S. Su, General atomic and molecular electronic structure system. *J. Comput. Chem.,* 14 (1993) 1347-1363.

[44] V. Nagarajan, R. Chandiramouli, TeO2 nanostructures as a NO2 sensor: DFT investigation. *Comput. Theor. Chem.,* 1049 (2014) 20-27.

[45] C. Tabtimsai, V. Ruangpornvisuti, B. Wanno, Density functional theory investigation of the VIIIB transition metal atoms deposited on (5, 5) single-walled carbon nanotubes. *Physica E: Low-dimensional Systems and Nanostructures,* 49 (2013) 61-67.

[46] W. Zhou, J. Zhou, J. Shen, C. Ouyang, S. Shi, First-principles study of high-capacity hydrogen storage on graphene with Li atoms. *J. Phys. Chem. Solids,* 73 (2012) 245-251.

[47] S. Mohammadi, M. Musavi, F. Abdollahzadeh, S. Babadoust, A. Hosseinian, Application of nanocatalysts in C-Te cross-coupling reactions: an overview. *Chem. Rev. Lett.,* 1 (2018) 49-55.

[48] J. Beheshtian, A.A. Peyghan, Z. Bagheri, Detection of phosgene by Sc-doped BN nanotubes: a DFT study. *Sens. Actuators. B,* 171 (2012) 846-852.

[49] M. Samadizadeh, S.F. Rastegar, A.A. Peyghan, F−, Cl−, Li+ and Na+ adsorption on AlN nanotube surface: a DFT study. *Physica E: Low-dimensional Systems and Nanostructures,* 69 (2015) 75-80.

[50] S. Kamalinahad, A. Soltanabadi, P. Gamallo, B 36 bowl-like structure as nanocarrier for sulfonamides: a theoretical study. *Monatsh. Chem.,* 151 (2020) 1785-1796.

[51] M. Ghiasi, S. Kamalinahad, M. Zahedi, Complexation of nanoscale enzyme inhibitor with carbonic anhydrase active center: A quantum mechanical approach. *Journal of Structural Chemistry,* 55 (2014) 1574-1586.

[52] M. Solimannejad, S. Kamalinahad, M. Noormohammadbeigi, H. Jouypazadeh, Chemisorption of pyrimidine nucleotide onto exterior surface of pristine B12N12 nanocluster: a theoretical study. *Physical Chemistry Research,* 6 (2018) 1-14.

[53] E. Pop, D. Mann, Q. Wang, K. Goodson, H. Dai, Thermal conductance of an individual single-wall carbon nanotube above room temperature. *Nano Lett.,* 6 (2006) 96-100.

[54] R.G. Parr, Density functional theory of atoms and molecules, Horizons of Quantum Chemistry: Proceedings of the Third International Congress of Quantum Chemistry Held at Kyoto, Japan, October 29-November 3, 1979, Springer, 1980, pp. 5-15.

[55] N.M. O'boyle, A.L. Tenderholt, K.M. Langner, Cclib: a library for package□independent computational chemistry algorithms. *J. Comput. Chem.,* 29 (2008) 839-845.

[56] S.F. Boys, F.d. Bernardi, The calculation of small molecular interactions by the differences of separate total energies. Some procedures with reduced errors. *Mol. Phys.,* 19 (1970) 553-566.

[57] A.E. Reed, R.B. Weinstock, F. Weinhold, Natural population analysis. *J. Chem. Phys.,* 83 (1985) 735-746.

[58] A. Redondo, Y. Zeiri, J.J. Low, W.A. Goddard III, Application of transition state theory to desorption from solid surfaces: Ammonia on Ni (111). *J. Chem. Phys.,* 79 (1983) 6410-6415.

[59] R. Kumar, N. Goel, M. Kumar, UV-activated MoS2 based fast and reversible NO2 sensor at room temperature. *ACS sensors,* 2 (2017) 1744-1752.

[60] A. Bano, J. Krishna, D.K. Pandey, N. Gaur, An ab initio study of sensing applications of MoB 2 monolayer: a potential gas sensor. *Phys. Chem. Chem. Phys.,* 21 (2019) 4633-4640.

[61] J. Li, Y. Lu, Q. Ye, M. Cinke, J. Han, M. Meyyappan, Carbon nanotube sensors for gas and organic vapor detection. *Nano Lett.,* 3 (2003) 929-933.

[62] N.L. Hadipour, A. Ahmadi Peyghan, H. Soleymanabadi, Theoretical study on the Al-doped ZnO nanoclusters for CO chemical sensors. *J. Phys. Chem. C,* 119 (2015) 6398-6404.